View metadata, citation and similar papers at core.ac.uk

brought to you by CORE

provided by HKU Scholars Hub

The HKU Scholars Hub The University of Hong Kong 香港大學學術庫

Title	**A simple, cost-effective but highly efficient system for deriving ventricular cardiomyocytes from human pluripotent stem cells**
Author(s)	**Weng, JZ; Karakikes, I; He, RJ; Kong, MCW; Ren, L; Geng, L; Chow, MZY; Keung, WWY; Hajjar, RJ; Li, RA**
Citation	**Stem Cell & Development, 2014**
Issued Date	**2014**
URL	**http://hdl.handle.net/10722/189344**
Rights	**Creative Commons: Attribution 3.0 Hong Kong License**

STEM CELLS AND DEVELOPMENT
Volume 00, Number 00, 2014
© Mary Ann Liebert, Inc.
DOI: 10.1089/scd.2013.0509

ORIGINAL RESEARCH REPORT

A Simple, Cost-Effective but Highly Efficient System for Deriving Ventricular Cardiomyocytes from Human Pluripotent Stem Cells

Zhihui Weng,[1,2] Chi-Wing Kong,[1,2] Lihuan Ren,[1,2] Ioannis Karakikes,[3] Lin Geng,[1,2] Jiaozi He,[1,4] Maggie Zi Ying Chow,[1,2] Chong Fai Mok,[1,2] Wendy Keung,[1,2] Howard Chow,[5] Anskar Y. H. Leung,[1,5] Roger J. Hajjar,[3] Ronald A. Li,[1–3,5] and Camie W. Chan[1,4,5]

Self-renewable human pluripotent stem cells (hPSCs) serve as a potential unlimited ex vivo source of human cardiomyocytes (CMs) for cell-based disease modeling and therapies. Although recent advances in directed differentiation protocols have enabled more efficient derivation of hPSC-derived CMs with an efficiency of ~50%–80% CMs and a final yield of ~1–20 CMs per starting undifferentiated hPSC, these protocols are often not readily transferrable across lines without first optimizing multiple parameters. Further, the resultant populations are undefined for chamber specificity or heterogeneous containing mixtures of atrial, ventricular (V), and pacemaker derivatives. Here we report a highly cost-effective and reproducibly efficient system for deriving hPSC-ventricular cardiomyocytes (VCMs) from all five human embryonic stem cell (HES2, H7, and H9) and human induced PSC (hiPSC) (reprogrammed from human adult peripheral blood $CD34^+$ cells using non-integrating episomal vectors) lines tested. Cardiogenic embryoid bodies could be formed by the sequential addition of BMP4, Rho kinase inhibitor, activin-A, and IWR-1. Spontaneously contracting clusters appeared as early as day 8. At day 16, up to 95% of cells were $cTnT^+$. Of which, 93%, 94%, 100%, 92%, and 92% of cardiac derivatives from HES2, H7, H9, and two iPSC lines, respectively, were VCMs as gauged by signature ventricular action potential and ionic currents ($I_{Na}{}^+/I_{Ca,L}{}^+/I_{Kr}{}^+/I_{KATP}{}^+$); Ca^{2+} transients showed positive chronotropic responses to β-adrenergic stimulation. Our simple, cost-effective protocol required the least amounts of reagents and time compared with others. While the purity and percentage of PSC-VCMs were comparable to a recently published protocol, the present yield and efficiency with a final output of up to 70 hPSC-VCMs per hPSC was up to 5-fold higher and without the need of performing line-specific optimization. These differences were discussed. The results may lead to mass production of hPSC-VCMs in bioreactors.

Introduction

SELF-RENEWABLE HUMAN (H) pluripotent stem cells (PSCs), including embryonic stem cells (ESCs) and induced PSCs (iPSCs), serve as a potential unlimited ex vivo source of human cardiomyocytes (CMs) for cell-based therapies, disease modeling, and other applications such as drug discovery and cardiotoxicity screening. Recent advances in directed cardiac differentiation protocols [1–7] have enabled the derivation of hESC/iPSC-CMs with yields several orders of magnitude higher than those of traditional methods, such as ''spontaneous'' embryoid body (EB) formation [8,9] and endodermal coculture [10,11]. Using defined serum-free media in combination with cocktails of such growth factors required for normal cardiogenesis as bone morphogenetic proteins (BMPs), activin-A, Wnt agonists and antagonists, fibroblast growth factor 2 (FGF2), and vascular endothelial growth factor (VEGF), and Dickkopf-related protein (DKK), these protocols can generate ~40%–90% cardiac troponin T $(cTnT)^+$ CMs with a final yield ranging from 1 to 20 CMs per starting undifferentiated hPSC [2–4,12,13]. However, they often require PSC-line-dependent titrations of multiple parameters (eg, BMP4 and activin-A concentrations) [1,14,15] and other specific needs (eg, sandwich matrix) [2], particularly for hiPSC lines that tend to be more variable [16]. Further, while relatively effective for generating cardiac cells, the resultant populations are undefined for chamber specificity [4,5,13] or heterogeneous containing mixtures of

[1]Stem Cell & Regenerative Medicine Consortium, LKS Faculty of Medicine, The University of Hong Kong, Pokfulam, Hong Kong.
[2]Department of Physiology, LKS Faculty of Medicine, The University of Hong Kong, Pokfulam, Hong Kong.
[3]Center of Cardiovascular Research, Mount Sinai School of Medicine, New York, New York.
[4]Department of Anatomy, LKS Faculty of Medicine, The University of Hong Kong, Pokfulam, Hong Kong.
[5]Department of Medicine, LKS Faculty of Medicine, The University of Hong Kong, Pokfulam, Hong Kong.

atrial, ventricular (V), and pacemaker derivatives [17]. Here we report a highly cost-effective and reproducibly efficient system for deriving hPSC-ventricular cardiomyocytes (VCMs) from all the five hESC (HES2, H7, and H9) and iPSC (reprogrammed from adult peripheral blood $CD34^+$ cells using non-integrating episomal vectors) lines tested.

Materials and Methods

hiPSC and ESC culture

hiPSC lines were derived from adult peripheral blood $CD34^+$ cells using the non-integrated episomal vectors pCXLE-hOCT3/4-shp53, pCXLE-hSK, and pCXLE-hUL [18]. Briefly, $CD34^+$ cells were purified (>95% purity) from anonymous donors and expanded in StemSpan™ H3000 (Stemcell Technologies) with the cytokine cocktail CC100 (Stemcell Technologies) for 3 days. Cells were nucleofected with the episomal vectors using the Human CD34 Cell Nucleofector™ kit (Amaxa) according to the manufacturer's protocol. After 72 h, cells were transferred to Matrigel™ (BD Biosciences)-coated plates in mTeSR™1 medium (STEMCELL Technologies). Morphological changes were observed a few days later. Colonies resembling hPSCs typically started to appear on day 7, and were picked on day 13 after nucleofection. H7 (WiCell), $H9^{DF}$, (a kind gift from Dr. Joseph Wu), HES2 (ESI) (passages 35–55) hESC and hiPSC lines were maintained in feeder- and serum-free condition in mTeSR1 medium on Matrigel at 37°C in 5% CO_2 in a humidified normoxic environment.

hiPSC validation

To characterize hiPSC clones, cultured cells were fixed by 4% paraformaldehyde in phosphate-buffered saline (PBS) for 15 min, followed by permeabilization by 0.1% Triton X-100 for 15 min, and washing with PBS for three times. The fixed samples were stained with anti-OCT4, SSEA-4, and Tra-1-81 for 2 h at room temperature (RT) (Supplementary Table S1; Supplementary Data are available online at www.liebertpub.com/scd) and then with flurochrome-conjugated goat anti-rabbit or anti-mouse secondary antibodies for 1 h. To test for pluripotency, hiPSCs were differentiated to form EBs in DMEM/F12 (Life Technologies) with 20% Knockout Serum Replacement (Life Technologies), 2 mM nonessential amino acids, 2 mM L-glutamine, and 0.1 mM β-mercaptoethanol. At day 15, EBs were stained for markers of the three germ layers (ie, Tuji, SMA, and AFP). For teratoma formation, 1×10^6 iPSCs were injected subcutaneously into NOD/SCID immunodeficient mice. Teratomas were harvested and stained 7–9 weeks after injection for H&E staining. Karyotyping was done according to a published protocol [19].

Direct ventricular cardiomyocyte differentiation

Undifferentiated hPSCs were digested into smaller clusters using Dispase (STEMCELL Technologies) and seeded onto Matrigel-coated plates at $\sim3\times10^5$ cells/10 cm^2 in mTeSR1 medium for 4 days until they were ~80%–90% confluence on D0 (Fig. 1). To initiate cardiac differentiation, hPSCs were digested into single-cell suspensions in ultra-low-attachment six-well plates (Corning) using Accutase (Invitrogen) and cultured in mTeSR1 medium with Matrigel (40 μg/mL) with BMP4 (1 ng/mL; Invitrogen) and Rho kinase inhibitor (ROCK) (10 μM; R&D) under a hypoxic condition with 5% O_2. Twenty-four hours later, the culture was washed and replaced in StemPro34 SFM (Invitrogen) with ascorbic acid (AA, 50 μg/mL; Sigma), 2 mM GlutaMAX-1 (Invitrogen), BMP4 (10 ng/mL), and human recombinant activin-A (10 ng/mL; Invitrogen) for 3 days. On day 4, IWR-1, a Wnt inhibitor (5 μM; Enzo Life Sciences), was added. Cardiac mesodermal cells developed into functional contracting clusters could be detected as early as day 8. On day 8, cells were transferred to a normoxic environment and maintained in StemPro34 SFM + AA medium for further characterization. In some cases, the cardiac mixtures (30–50 days old) were transduced with the recombinant lentivirus (LV)-MLC2v-Tdtomato-T2A-Zeo. MLC2v-positive cells were selected using the antibiotic Zeocin.

Immunostaining for CMs and flow cytometry analysis

For immunostaining of cardiac cells, beating clusters (between 16 and 35 days of differentiation) were digested into single cells and immunostained with anti-cTnT, sarcomeric, α-actinin, connexin 43, COXIV, myosin heavy chain (MF20), two isoforms of myosin light chain 2, MLC2a, and MLC2v antibodies listed in Supplementary Table S1. Primary antibodies were diluted in PBS with 1% BSA and incubated at RT for 2 h. Alexa Fluor (AF)488-conjugated goat anti-mouse IgG or AF555 anti-mouse IgG (Invitrogen) were used as secondary antibodies and stained for 1 h at RT. Coverslips were mounted onto glass slides in Prolong Gold mounting medium with DAPI (Invitrogen) and samples were imaged on LSM Carl Zeiss 510 Meta (Carl Zeiss) or Nikon Eclipse TiS microscope. For flow cytometry, cells were digested and resuspended in PBS with 2% FBS. To stain for intracellular markers, cells were fixed, permeabilized, and stained with antibodies against various cardiac markers. To measure cardiac differentiation, percentages of CMs were estimated based on the % of cTnT-positive cells at differentiation days 16–18.

Metabolic stress and mitochondrial membrane potential

Mitochondrial membrane potential in HES2-VCMs was measured with the potential-sensitive dye JC-1 (Invitrogen). LV-MLC2v-Tdtomato-T2A-Zeo–transduced and Zeo-selected HES2-VCMs (30–50 days old) were incubated at 37°C with 0.5 μM JC-1 in serum-free DMEM for 15 min. To simulate metabolic oxidative stress, HES2-VCMs were treated with hydrogen peroxide (H_2O_2; 100 μM) for 30 min at 37°C after which JC-1 orange and green fluorescence intensity was measured for mitochondrial membrane potential with LSM Carl Zeiss 510 Meta.

Mitochondrial volume estimation

HES2-VCMs were incubated at 37°C with 0.1 μM MitoTracker® Deep Red and 0.1 μM Cell Tracker (Invitrogen) for 30 min for mitochondrial volume estimation. Stack images of mitochondria and cytoplasm were obtained with LSM Carl Zeiss 510 Meta. Three-dimensional images of HES2-VCMs were constructed and mitochondrial volume

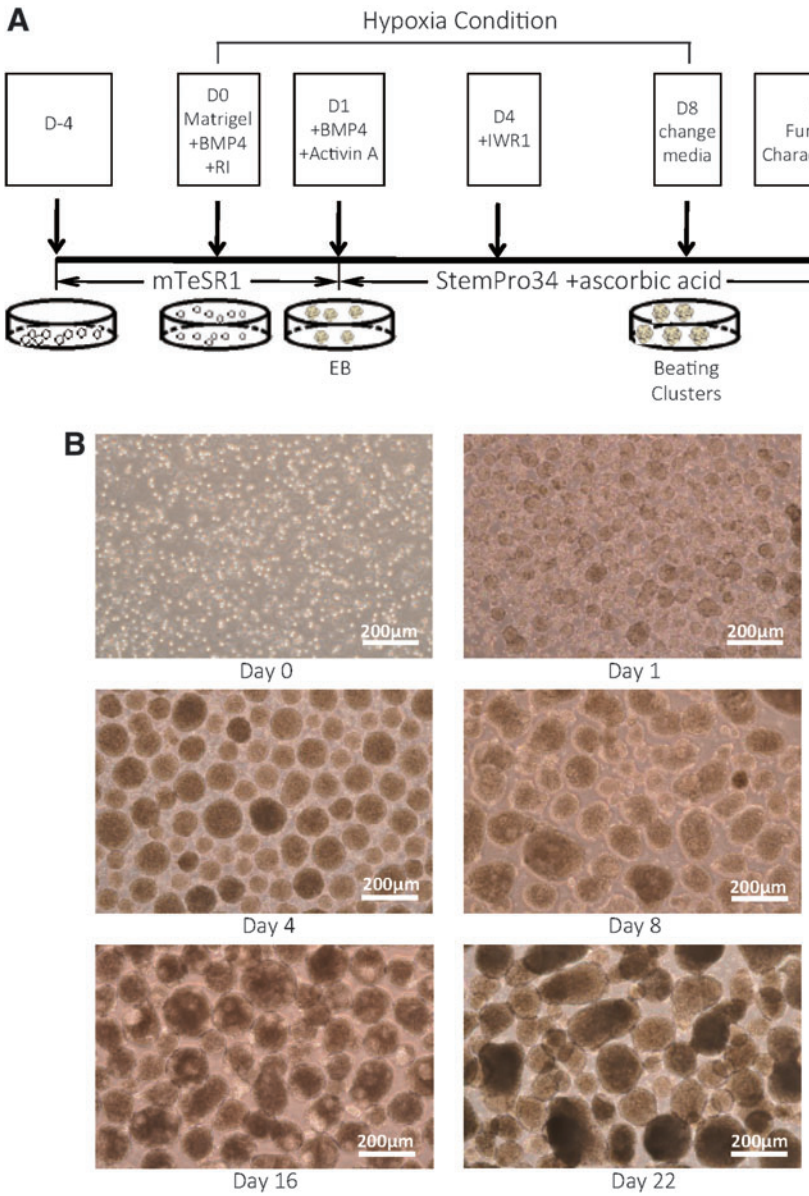

FIG. 1. A highly efficient ventricular cardiomyocyte (VCM) differentiation system of human pluripotent stem cells (hPSCs). **(A)** Schematic of a direct differentiation protocol used for the differentiation of hPSCs to VCMs under non-feeder and non-xenogeneic conditions. Spontaneously contracting clusters were detected as early as day 8. **(B)** Images demonstrate typical culture morphology at different time points of differentiation. Scale bar = 200 µm. Color images available online at www.liebertpub.com/scd

was estimated as % of total cell volume with the imaging analysis software Imaris (Bitplane).

RNA extraction, cDNA synthesis, and gene expression analysis by real-time PCR

Total RNA was extracted from samples using RNeasy Mini Kit (Qiagen) following DNase I (Promega) treatment for the removal of potential contamination of genomic DNA. cDNA was prepared using the QuantiTect Rev. Transcription Kit (Qiagen) following the manufacturer's protocol. Gene expression was quantified using StepOnePlus™ Real-Time PCR system (Applied Biosystems). PCR amplification was carried out in 96-well optical plates consisting of 100 ng of cDNA template, 5 pmol of forward and reverse primers, and 1X KAPA SYBR® Fast qPCR Master Mix (KAPA Biosystems). The reactions were incubated at 95°C for 3 min, and followed by 40 cycles of 95°C for 3 s, and 60°C for 20 s. GAPDH was used as internal control to normalize loading and all reactions were performed in triplicate. Primers are listed in Supplementary Table S2.

Electrophysiological characterization

Electrophysiological experiments were performed using the whole-cell patch-clamp technique as previously described [20–22]. To profile chamber-specific subtypes of our hPSC-derived CMs (hPSC-CMs), action potentials (APs) of the myocytes were randomly probed at 37°C with the patch-clamp technique using an EPC-10 amplifier and Pulse software (Heka Elektronik), with the current-clamp mode (0.1–0.5 nA for 1–5 ms) under the whole-cell configuration applied. The hPSC-CMs were categorized into nodal, atrial, or ventricular like according to the standard AP parameters as we and others previously described [17,20,21]. Voltage-clamp recordings of ionic currents were performed using an automated parallel patch-clamp system (PatchXpress 7000A; Molecular Devices) using standard electrophysiological and

pharmacological protocols for isolating the ionic component of interest (see Supplementary Data for details).

Ca^{2+} imaging

The intracellular Ca^{2+} ($[Ca^{2+}]_i$) transients were imaged by a spinning disc laser confocal microscope (PerkinElmer) on hPSC-CMs loaded with 1.5 μM X-Rhod-1 (Invitrogen) as previously described [21]. After dye loading, experiments were performed at 37°C in Tyrode's solution containing 140 mM NaCl, 5 mM KCl, 1 mM $MgCl_2$, 1.25 mM $CaCl_2$, 10 mM HEPES, and 10 mM D-glucose at pH 7.4. Electric pulses (40 ms pulse duration; 40 V/cm; 1 Hz) generated by a field generator were continuously applied to pace electrically induced Ca^{2+} transients ($E[Ca^{2+}]_i$). The amplitudes of $E[Ca^{2+}]_i$ are presented as the background-corrected pseudo ratio $(\Delta F/F) = (F - F_{base})/(F_{base} - B)$ where F_{base} and F are the measured fluorescence intensity before and after stimulation, respectively, and B is the average background signal from areas adjacent to the targeted cell. The transient rise ($V_{upstroke}$) and the transient decay (V_{decay}) were subsequently calculated and analyzed.

Transplantation and in vivo tracking of hESC-VCMs

$H9^{DF}$ cells stably expressing a double-fusion reporter gene consisting of firefly luciferase and enhanced GFP [23,24] were a kind gift from Dr. Joseph Wu and used for in vivo monitoring of CM survival. Specifically, $2–3 \times 10^5$ $H9^{DF}$-CMs were transplanted to the kidney capsule of NOD.Cg-Prkdc^{scid}Il2rg^{tm1Wjl}/SzJ mice (6–10 weeks old). Transplanted cell survival was longitudinally monitored via bioluminescence imaging (BLI) using the Xenogen in vivo imaging system (Caliper Life Sciences). Briefly, mice were anesthetized with isoflurane and D-Luciferin (Invitrogen) was administrated intraperitoneally at a dose of 375 mg/kg of body weight. BLI signal was measured in maximum photons per sec per centimeter square per steradian (p/s/cm^2/sr). All procedures performed were approved by the Committee on the Use of Live Animals in Teaching and Research at the University of Hong Kong. For detection of the transplanted CMs, animals were killed at different time points and kidneys were harvested and stained for the presence of cTnT-positive cells (see Supplementary Data for details).

Statistical analysis

Data are presented as means ± SEM. Student's *t*-test or ANOVA was used to measure statistical significance. $P < 0.05$ is considered significant.

Results

Highly efficient ventricular specification of hESCs

We initially focused on HES2, the same hESC line that Keller et al. employed for developing their original directed differentiation protocols [1,3,25]. Our modified method for ventricular specification is schematically summarized in Figure 1A. To start, undifferentiated cells were seeded as 30,000 cells/cm^2 for expansion in mTeSR1 medium for 4 days. On day 0, hPSCs were digested into single cells and cultured in suspension in mTeSR1 medium with Matrigel along with BMP4 (1 ng/mL) and ROCK (10 μM) to induce differentiation. After 24 h, the media was changed to StemPro34 SFM with BMP4 (10 ng/mL), activin-A (10 ng/mL), and AA (50 μg/mL) to induce the formation of cardiogenic mesodermal EBs. As the last step, on day 4 when nicely compact rounded aggregates could be observed, IWR-1 (5 μM) was added to suppress Wnt signaling (Fig. 1B). As early as day 8, >70% of hEBs from 30 out of 30 independent differentiation reactions became spontaneously contracting (eg, vs. ~50% on days 10–12 of Keller [3]; see Supplementary Video S1 and S2). On days 16–18, ~100% of hEBs were beating and, for the cTnT-positive cells, about 17% were Ki67-positive proliferating (Supplementary Fig. S1).

As anticipated, using real-time RT-PCR analysis, we detected that the transcript expression of the pluripotency markers *OCT4* and *Nanog* decreased time dependently, and rapidly became undetectable by days 4–5 (Fig. 2). By contrast, the transcript expression of T-box factor Brachyury (T) and helix-loop-helix transcription factor mesoderm posterior 1 (MESP1), one of the earliest ''cardiac'' mesoderm markers, transiently spiked during days 2–5 upon the addition of BMP4 and activin-A. During the same time interval, the cardiac progenitor marker *Isl1* as well as the transcription factors *GATA4* and *Hand1*, critical for early cardiac differentiation, also became expressed, with the early cardiac progenitor marker *Nkx2.5* appearing shortly after on d5 (after IWR addition), peaked at day 8, and continued to remain high beyond day 14. Consistent with a successful cardiac differentiation, further analyses revealed that transcripts of sarcomeric proteins, such as *MYH6*, *MYH7*, *cTnT*, and *NPPA*, that are signatures of contractile CMs also had similar time-dependent expression patterns. Expression levels of *ML2Cv*, a marker of mature ventricular CMs, increased to a high level at day 16 and remained so over 30 days. By contrast, the expression of *MLC2a*, which is normally expressed in atrial and immature ventricular CMs, peaked at day 16 and declined afterward. The temporal transcript expression profiles of the various pluripotency, mesodermal, and cardiac makers are summarized in Figure 2.

hESC-CMs displayed a time-dependent switch from MLC2a to MLC2v positive

To quantitate the efficiency of our specification protocol, flow cytometry analysis was performed on differentiated HES2 cells collected at days 16–18. As depicted in Figure 3A, the yield of $cTnT^+$ cells was 90.8% for the representative reaction shown with an average of 87% ± 3.4% for the HES2 line ($n = 6$ independent reactions; Fig. 3B). Immunostaining experiments confirmed the subcellular expression of cardiac-specific proteins (ie, MLC2v, MLC2a, MF20, α-actinin, and connexin 43) with the expected sarcomeric structures (Fig. 4A), indicating that the derived cells were hESC-CMs. As shown in Figure 4B, by day 20, ~85% of the differentiated cells were positively stained for ML2Cv. Consistent with our qRT-PCR data, only ~35% of the MLC2v-positive cells were also positive for MLC2a (Fig. 4B). By day 40, essentially all of HES2-VCMs did not express MLC2a but only MLC2v (Fig. 4C), signifying that the VCMs derived were amenable to maturation in vitro. Considering the input of 300,000 hESCs at day 4, the output

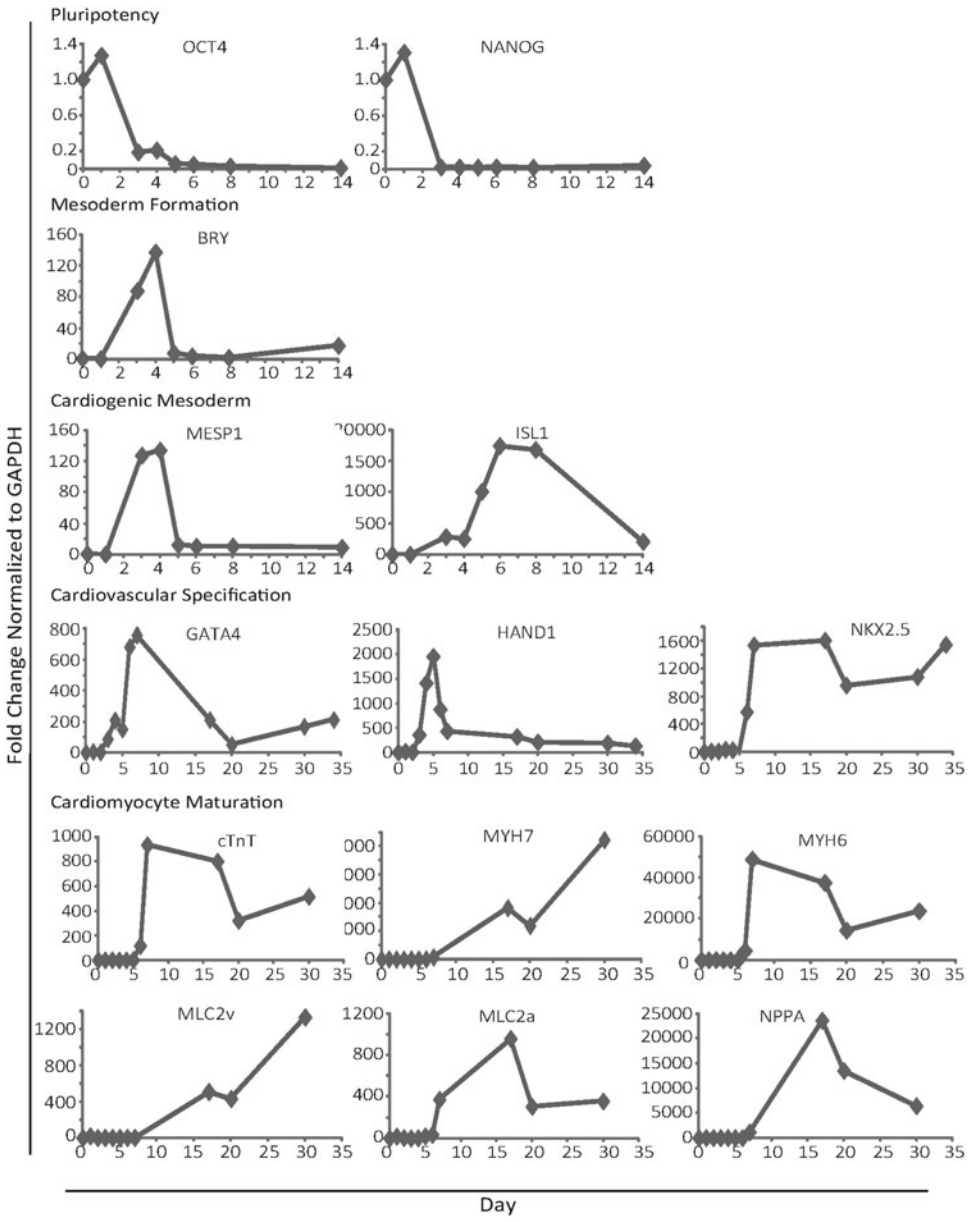

FIG. 2. Quantitative PCR-based gene expression analysis of embryoid bodies (EBs) at different stages of cardiac differentiation. HES2 were subjected to the cardiac differentiation protocol described in Figure 1. Expression levels of pluripotent, cardiac mesoderm markers, and cardiac specific genes were normalized and expressed relative to housekeeping gene GAPDH. Plots shown are representative of three independent experiments.

of our protocol as determined by flow cytometry was ~32–72 cTnT-positive cells per HES2 cell at day 14.

Functional characterization of hESC-VCMs

To confirm the functionality as well as chamber-specific identity of our derived CMs, we next performed patch-clamp recordings and Ca^{2+} imaging on 35–50-day-old single cells isolated from cardiogenic EBs for examining their electrophysiological profiles. Of the 42 HES2-CMs recorded (from five independent batches), 93% displayed an AP profile that was most consistent with the immature ventricular type that we had previously published [17,21,26] (Fig. 5A, D). Immature traits such as spontaneous AP firing, a depolarized resting membrane potential or maximum diastolic potential, and phase 4 depolarization were readily observed. AP parameters are summarized in Table 1. Consistent with AP data, when unselected cells isolated from HES2-EBs were immunostained with MLC2v and cTnT, >80% of the cells were doubly MLC2v and cTnT positive, suggesting that our method supports a high percentage of VCM differentiation (Fig. 5B). After zeocin selection, 100% of LV-MLC2v-Tdtomato-T2A-zeocin–transduced cells displayed typical ventricular-like APs. Therefore, the cells derived by our protocol were functional hESC-VCMs. As for Ca^{2+} handling, Figure 5C shows that transients from these cells had amplitudes and kinetics smaller and slower than those of adults as we previously reported [27,28]. Further, caffeine-induced Ca^{2+} was also observed, indicating a functional sarcoplasmic reticulum. Upon isoproterenol (Iso) application to our hESC-VCMs, a positive chronotropic response with increased spontaneous AP and Ca^{2+} transient firings was observed. However, the transient amplitude remained unchanged ($P > 0.05$), indicating a null ionotropic response to β-adrenergic stimulation. Moreover, a live recording of the electrically induced Ca^{2+} transient

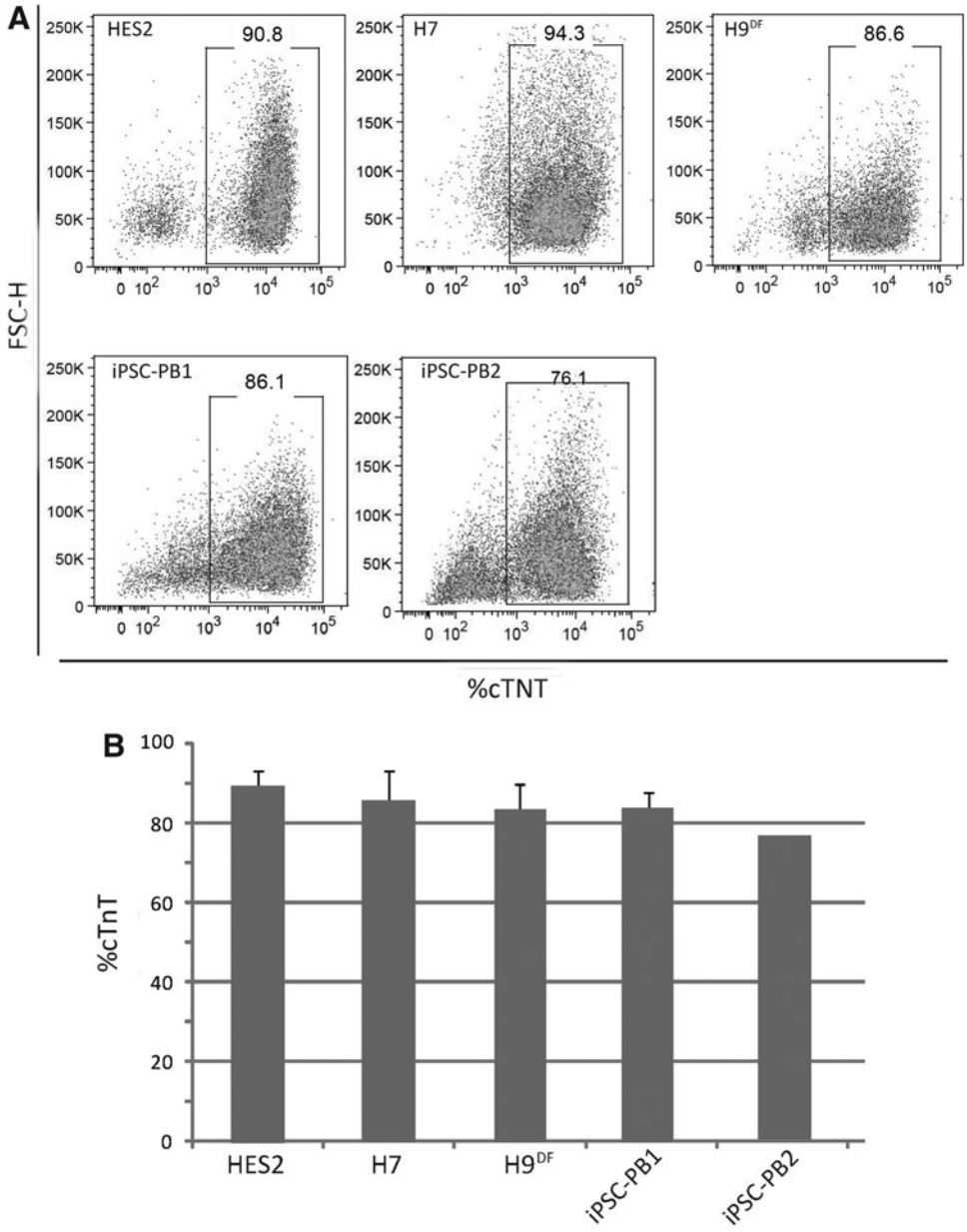

FIG. 3. Specification of cardiac differentiation in multiple hPSC lines. **(A)** Representative flow cytometry plots of cardiac troponin T $(cTNT)^+$ cells differentiated from hPSCs. The entire well of one 6-well plate was enzymatically digested into a single-cell suspension and 100,000 cells were analyzed. **(B)** Percentages of $cTnT^+$ cells in day 16–18 EBs of HES2, H7, $H9^{DF}$, and two nonviral $CD34^+$-derived human induced PSC (hiPSC) lines. Mean ± SEM.

(Supplementary Video S3) recorded from a culture of iPSC-CM also indicated the functional Ca^{2+} handling in the CMs. When switched to the voltage-clamp mode, signature ventricular ionic currents, such as voltage-dependent I_{Na}, L-type I_{Ca}, I_{Kr}, sarcolemmal I_{KATP}, could be recorded (Fig. 6), electrophysiologically confirming the identity as VCMs.

Immature mitochondrial structure of HES2-VCMs

Others have reported that the structure of mitochondria reflects various stages of cardiogenesis [29,30]. At day 30 post-differentiation, similar to embryonic/fetal CMs, HES2-VCMs displayed a perinuclear mitochondrial structure, as shown by staining with the mitochondrial COXIV-specific antibody (Fig. 7A). In addition, the mitochondrial volume of HES2-VCMs was 33.7% ± 0.4% ($n = 16$) at day 30, smaller than the reported value of 40% in human adult CMs [31]. Therefore, HES2-VCMs were more comparable to fetal CMs that also carry a lower mitochondrial mass with perinuclear localization compared with adult CMs [32]. We next examined the mitochondrial inner membrane potential of HES2-VCMs using the potential-sensitive JC-1 dye. Figure 7B shows the appearance of both green and red fluorescence HES2-VCMs, demonstrating the presence of both depolarized (green monomer) and hyperpolarized (orange aggregate) mitochondrial membrane potential. Areas of depolarized mitochondrial membrane potential were found in the perinuclear region while areas of hyperpolarized potential were mainly found at the perimeter of HES2-VCMs. Similar to primary CMs, when subjected to oxidative stress in the form of H_2O_2, hESC-VCMs showed a depolarization of their mitochondrial membrane potential (increase in green vs. orange fluorescence) with JC-1 orange/green intensity ratio decreased from 1.146 to 0.410.

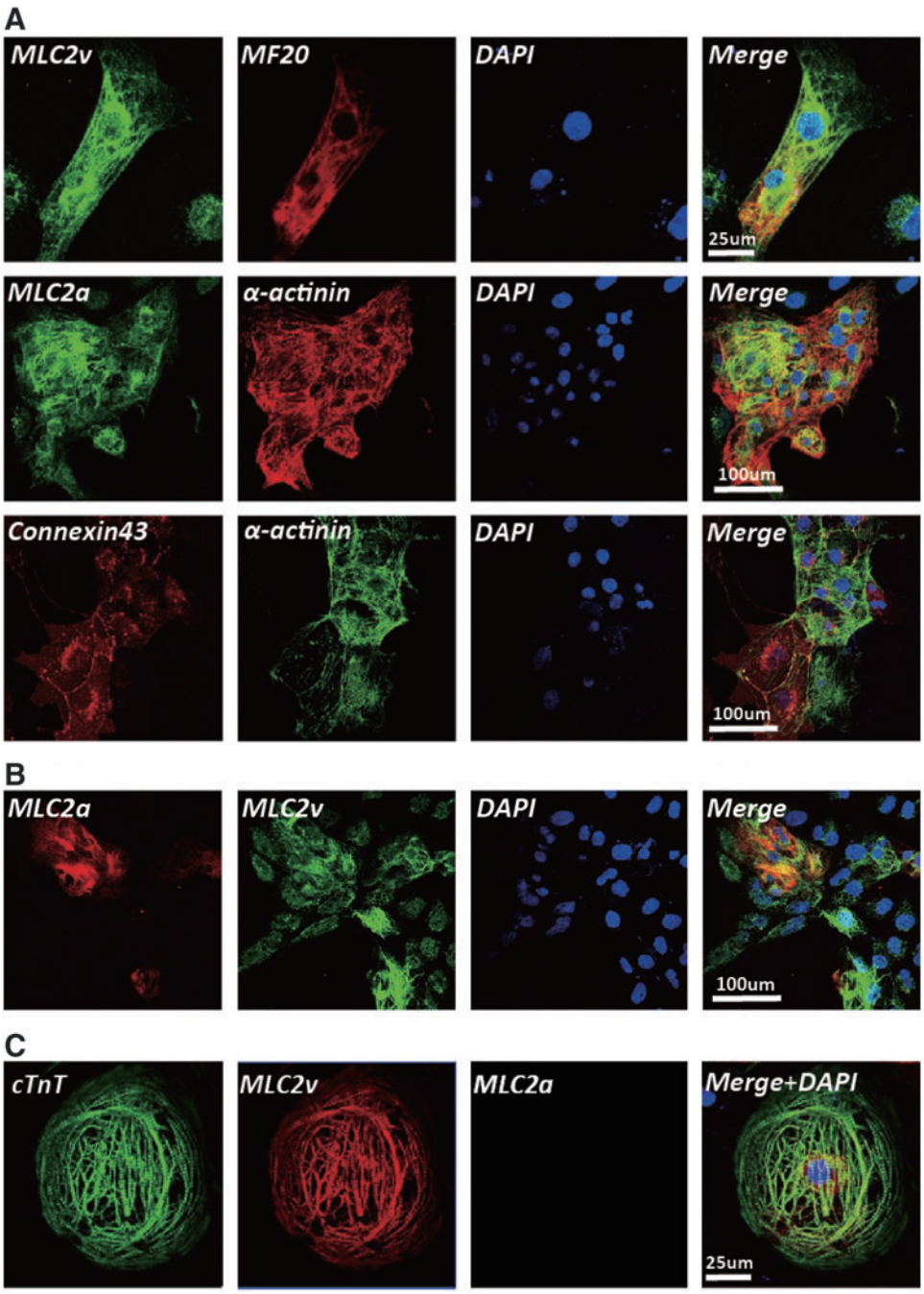

FIG. 4. Structural characterization of HES2-cardiomyocyte (CM) by immunostaining. **(A)** HES2-EBs were digested into single cells at day 20 of differentiation and then costained for MLC2v/MF20, MLC2a/α-actinin, and connexin 43/α-actinin. Nuclei were counterstained with DAPI (*blue*). Representative immunostaining images for MLC2a and MLC2v in HES2-CMs examined at **(B)** day 20 and **(C)** day 40 postdifferentiation. Color images available online at www.liebertpub.com/scd

Ventricular specification of additional hESC lines and hiPSCs reprogrammed from human CD34$^+$ cells

Given that most methods for directed cardiac differentiation reported to date require line-dependent optimizations of growth factors [1,3,4,15], we next tested the versatility of our protocol for consistent hPSC-VCM yields with different lines. Indeed, we have previously reported that distinct hESC lines have different cardiogenic potentials [33]. Such differences can be further exemplified in hiPSCs, which are known to display significant line-to-line and clone-to-clone variability. Therefore, we generated hiPSCs from adult peripheral blood CD34$^+$ cells using non-viral episomal vectors (see Materials and Methods section). All our tested hiPSC lines retained a normal karyotype, stained positively for pluripotency markers by immunocytochemistry, and expressed high levels of Oct4 and Rex1 (data not shown). Differentiation into three germ layers was confirmed by qRT-PCR and immunostaining. When injected subcutaneously into the immunodeficient mice, all tested hiPSC lines formed teratomas consisting of the three primitive germ layers (Supplementary Fig. S2). When these hiPSC lines were subjected to ventricular specification by our protocols,

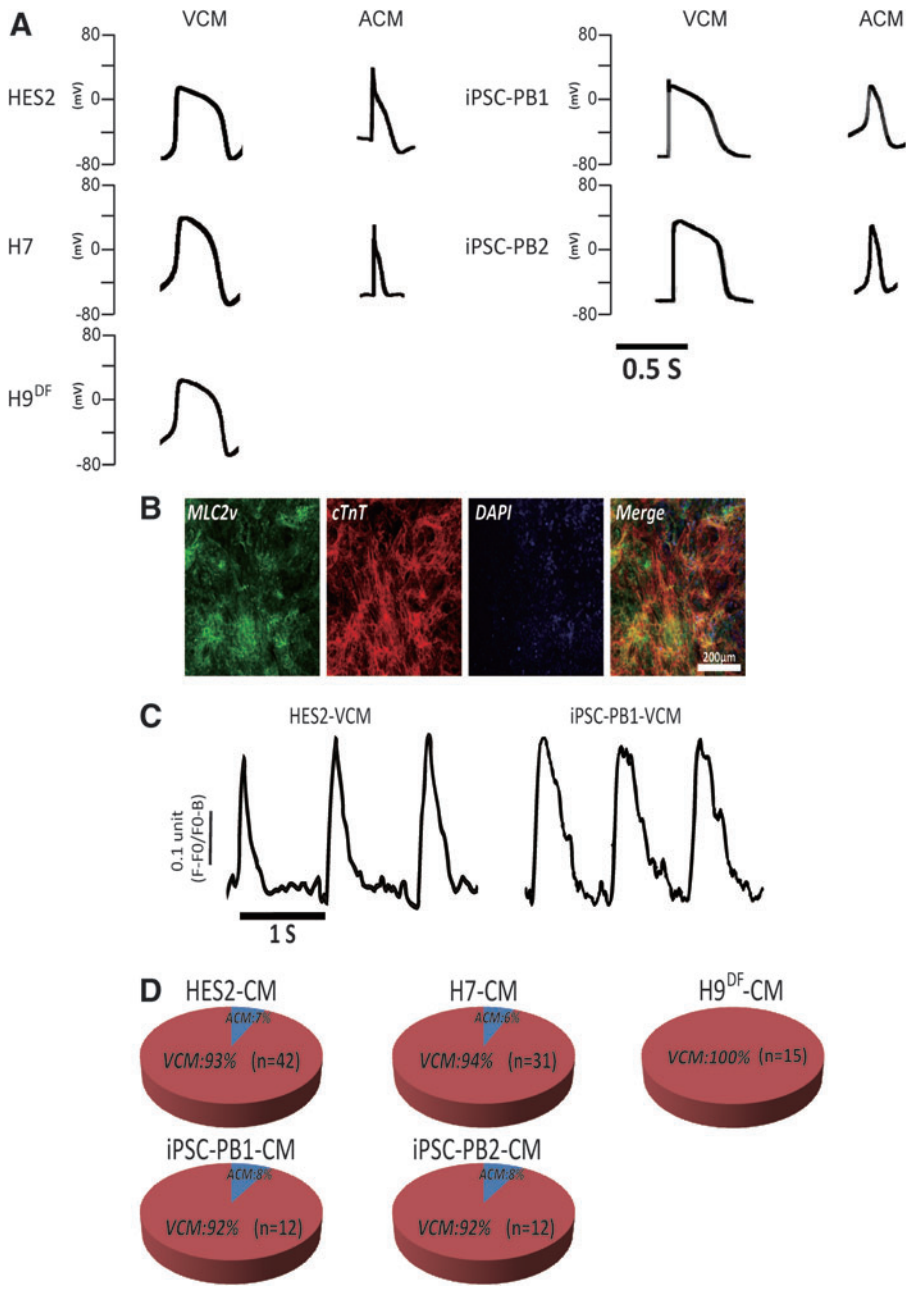

FIG. 5. Specification of ventricular differentiation of hPSCs. **(A)** Representative action potential (AP) profiles of HES2-CMs, H7-CMs, $H9^{DF}$-CMs, iPSC-PB1-CMs, and iPSC-PB2-CMs measured by patch-clamp recordings. **(B)** Immunostaining of nonselected HES2-CMs for MLC2v and cTnT expression. HES2-EBs were digested into single cells and then reseeded for immunostaining without any purification. Scale bar = 200 μm. **(C)** Representative Ca^{2+} transient tracings of HES2-VCMs and iPSC-PB1-VCMs paced by electrical field stimulation (1 Hz, 40 V/cm). All cells examined were > 35 days old. **(D)** Percentages of cells expressing VCM and atrial cardiomyocyte (ACM) AP profiles as detected by patch-clamping. Color images available online at www.liebertpub.com/scd

spontaneously contracting cardiogenic EBs routinely emerged on days 8–9 and achieved ~80% $cTnT^+$ cells (Fig. 3), which likewise expressed the cardiac markers cTnT, α-actinin, and MLC2a with immature signature ventricular AP and Ca^{2+} transients (Fig. 5). When tested with additional hESC lines, H7 and $H9^{DF}$, qualitatively similar data in terms of time when beating EBs first appeared, % of $cTnT^+$ cells, APs, and Ca^{2+} transients were also consistently observed (Figs. 3 and 5). Taken collectively, the yield of VCMs ranged 92%–100% as gauged by APs (Fig. 5G). The remainders were atrail-like hPSC-CMs (Fig. 5A). We did not detect any nodal-like hPSC-CMs.

TABLE 1. SUMMARIZATION OF THE ACTION POTENTIAL PROPERTIES OF HES2-VCMS ($N = 2$)

Firing frequency (Hz)	*Amplitude (mV)*	*Upstroke velocity (mV/ms)*	*Decay velocity (mV/ms)*	*APD50 (ms)*	*APD90 (ms)*	*MDP (mV)*
1.59 ± 0.03	94.0 ± 0.4	8.85 ± 0.31	−0.76 ± 0.01	443.0 ± 8.4	571.4 ± 9.0	−72.5 ± 0.2

VCMs, ventricular cardiomyocytes.

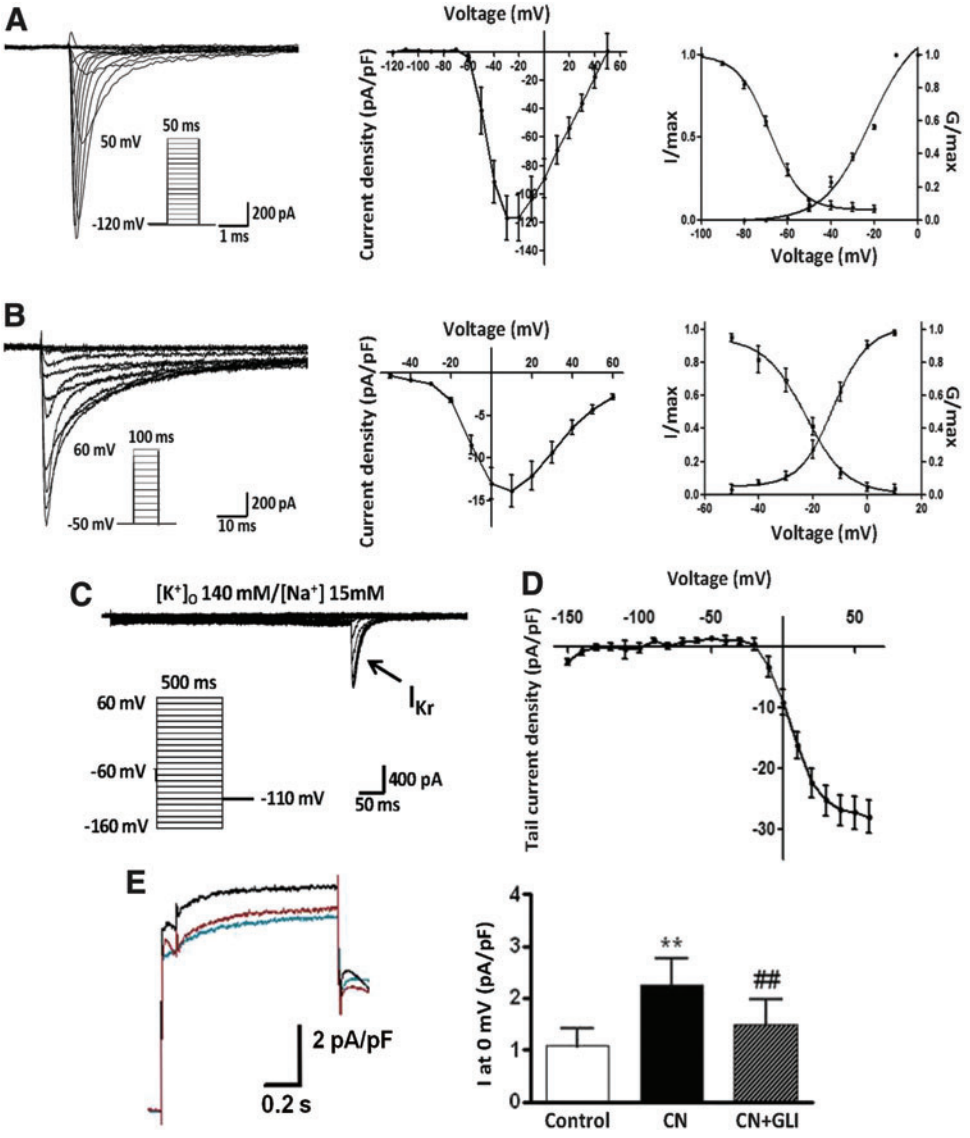

FIG. 6. Ionic currents (I_{Na}, I_{CaL}, I_{Kr}, and I_{KATP}) in HES2-CMs. Representative **(A)** I_{Na} and **(B)** I_{CaL} traces elicited by voltage protocol shown in *inset*. *Middle:* peak I–V plots. *Right:* Steady-state inactivation and activation relations. ($n=7$). **(C)** Representative I_{Kr} traces after the subtraction of E4031-insensitive current elicited by voltage protocol shown in *inset*. **(D)** Activation relation of I_{kr} ($n=11$). **(E)** Sarcolemmal I_{KATP} channels in HES2-VCMs. *Left panel:* representative tracings of sarcolemmal I_{KATP} in HES2-VCMs at 0 mV under control conditions (*blue line*), with sodium cyanide (CN, 2 mM) alone (*black line*), or with CN and glibenclamide (GLI, 10 μM; *red line*). *Right panel:* summary of averaged current densities under the same conditions. Cells were stimulated to 0 mV for 1,000 ms from a holding potential of −80 mV preceded by a 100-ms prepulse to −10 mV ($n=5$). $^{**}P<0.01$ compared with control group; $^{\#\#}P<0.01$ compared with CN group. Color images available online at www.liebertpub.com/scd

Transplantation of hPSC-VCMs for in vivo studies

Previous transplantation studies of hESC-CMs almost always involved cell mixtures with low yields of hESC-CMs or heterogenous mixtures of V and other chamber-specific types [24,34]. To test the in vivo survival of our hPSC-VCMs, we employed our protocol to differentiate a H9 cell line expressing the double-fusion GFP-luciferase proteins to H9-VCMs [24]. Figure 8A shows that >72% of $cTnT^+$ cells could be generated. After transplantation into the kidney capsule of immunodeficient mice, $cTnT^+$ cells remained detected for least 27 days (Fig. 8B, C). Immunohistochemistry staining showed a localized region of cTnT-positive cells in the transplanted kidney capsule (Fig. 8D). Therefore, our robust differentiation of VCMs of hPSCs provides a great cell source for future transplantation experiments.

Discussion

In the present study, we have made the following salient accomplishments: (i) a final output of ~35–70 hPSC-VCMs per hPSC (vs. 1–20 hPSC-CMs per hPSC, of which merely a fraction was VCMs); (ii) a relatively simple and cost-effective protocol that reproducibly generates cardiac cells within a short time and requires the least amounts of reagents (eg, bFGF and VEGF were not needed for expansion); (iii) the protocol is effective for multiple hESC and hiPSC lines without the need of line-dependent optimization; and (iv) ventricular specification of hESC/iPSCs, as confirmed electrophysiologically by ventricular AP and ionic currents. These results are further discussed in the following headings in relation other recent relevant studies.

Comparison with other directed cardiac differentiation protocols

Recent advances in directed cardiac differentiation protocols have enabled the derivation of hESC/iPSC-CMs in larger quantities. These protocols have generally adopted the approach of sequential addition of growth factors. The first major breakthrough was accomplished by Yang et al.

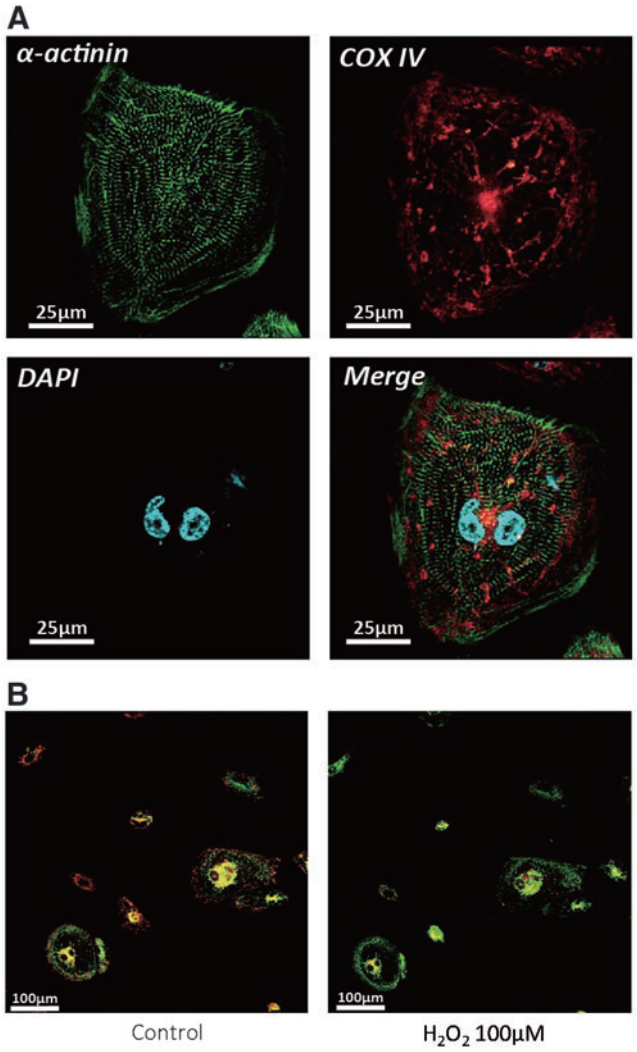

FIG. 7. Immature mitochondrial structure of HES2-VCMs. **(A)** Lentivirus (LV)-MLC2v-Tdtomato-T2A-Zeo–transduced and Zeo-selected HES2-VCMs (30–50 days old) were immunostained for α-actinin and mitochondrial cytochrome c oxidase (COX)IV. Nuclei were counterstained with DAPI (*blue*). Scale bar = 25 μm. **(B)** HES2-VCMs were stained using the potential-sensitive JC-1 dye. *Left panel* shows representative image of control cells with both *green* and *red* fluorescence in the HES2-VCMs. *Right panel* shows representative image of HES2-VCMs subjected to 100 μM hydrogen peroxide (H_2O_2) ($n = 3$). Scale bar = 100 μm. Color images available online at www.liebertpub.com/scd

who developed a directed differentiation protocol of deriving hESC (HES2)-CMs via stage-specific addition of a combination of activin-A, BMP4, FGF2, VEGF, and Dickkopf-1 (DKK-1) to generate a tripotent cardiovascular progenitor population [3]. The method requires optimization on the growth factor concentrations for different specific PSC lines with the reported yield of >50% of beating clusters. Using this protocol, we could differentiate ~40% of $cTnT^+$ cells from HES2 cells, which heterogeneously consisted of a mixture of ventricular, atrial, and pacemaker derivatives (with a ratio of 42:53:5) [26]. The total output is therefore ~4 hPSC-CMs or 2.2 hPSC-VCMs per hPSC.

Burridge et al. optimized >45 experimental variables to develop a protocol with optimized concentrations of BMP4 and FGF2, polyvinyl alcohol, serum, and insulin for cardiac differentiation of hESCs (H1 and H9) and hiPSC lines derived from neonatal $CD34^+$ CBs (CBiPSC6.2 and CBiPSC6.11) and adult fibroblasts (iPS-IMR90-1) using nonintegrated episomal plasmids to generate 64%–89% $cTnT^+$ cells by day 9 [4]. The derived CMs are functionally responsive to cardioactive drugs when optically mapped as multicellular clusters. However, the efficiency and AP profiles and distribution of the differentiated CMs were not mentioned.

In the study by Lian et al., the investigators employ glycogen synthase kinase 3 (GSK3) inhibitors combined with the β-catenin shRNA or a chemical Wnt inhibitor to produce a 80%–98% purity of functional CMs in 14 days from hESCs (H9, H13, and H14) and multiple hiPSC lines (6-9-9, 19-9-11, and IMR90C4) [12]. Similar to our findings reported here, beating clusters are observed between days 8 and 10. About 20% of day-20 CMs are proliferative as indicated by Ki67 staining or BrdU assay. The number of cells generated by this protocol is 15 CMs per hPSC input without any enrichment and/or purification step. The method focuses on early induction of canonical Wnt signaling and suppression of canonical Wnt signaling at later stages of differentiation to synergistically enhance the CM yield.

Zhang et al. reported a matrix sandwich method by overlaying monolayer-cultured hPSCs with Matrigel [2]. They combined the matrix sandwich with sequential application of activin-A, BMP4, and bFGF to generate a high purity of up to 98% and a yield of up to 11 CMs/input PSC from multiple PSC lines, including H1, H9, and three iPSC lines derived from foreskin fibroblasts using nonintegrating vectors and the lentiviral-generated iPS cell line IMR90 clone 4 (IMR90 C4). Atrial/ventricular distribution is not reported.

Ren et al. reported early modulation of the BMP4 coupled with late inhibition of Wnt signaling pathways in hiPSCs to generate high efficiency of cardiac differentiation [14]. This method, tested on H7 only, requires a high concentration of serum (20%) but with a relatively low percentage of cTNT-positive cells (~16%). AP profile is also not reported. Minami et al. reported the use of a single small-molecule KY02111 to promote hPSC differentiation into CMs with a yield of up to 98% by inhibiting WNT signaling [13]. EP data show that VCMs and pacemaker cells are present and electrophysiologically functional. The method, tested on four hiPSC lines, can be achieved in a serum- and xeno-free condition to produce $\sim 4.2 \times 10^6$ hPSC-CMs from ~6 to $\times 10^6$ seeded initially per well or 0.7 hPSC-CMs per hPSC. Given that this method requires only a single small molecule to direct CM differentiation, it is by far the simplest protocol. The ventricular yield is unknown.

Comparison with our recent ventricular specification protocol

The present method differs from our recently published protocol [35] in several ways. First, here we used ROCK and Matrigel instead of Blebbistatin on day 0. Second, 10-fold less of BMP4 was used on day 0 and 2.5-fold less of activin-A was added on day 1 in our protocol. Third, our cells were digested by Accutase into single cells on day 0, as

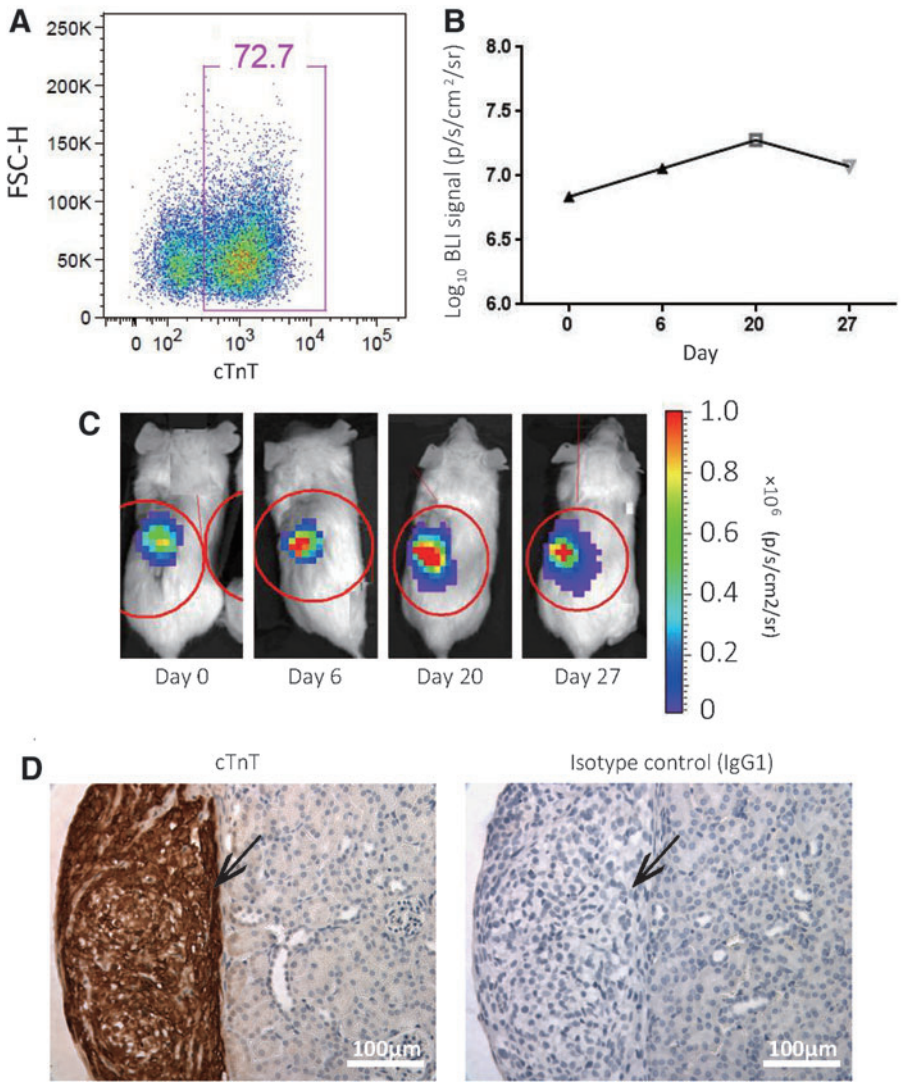

FIG. 8. In vivo survival of H9-VCMs under kidney capsule transplantation. **(A)** $H9^{DF}$ was used to differentiate VCMs. Differentiation efficiency was estimated based on cTnT protein expression by flow cytometry. Representative FACS plot is shown. **(B)** In vivo bioluminescence imaging (BLI) signal measured from animals in which $H9^{DF}$-VCMs were transplanted into the kidney capsule. **(C)** A representative animal imaged following transplantation of 2×10^5 $H9^{DF}$-VCMs into the kidney capsule. Color scale bar value represents photons/sec/cm^2/steradian (p/s/cm^2/sr). **(D)** Immunohistochemistry for cTNT-positive cells in the transplanted kidneys harvested on d28. Scale bar = 100 μm. Color images available online at www.liebertpub.com/scd

opposed to small clusters in the other protocol. Fourth, there was no media change on day 3, instead of changing to StemPro + AA with IWR on day 4. Fifth, IWR-1 was added on day 4 at 5 μM, instead of 2.5 μM on day 4.5. Finally, our cells were maintained in normoxia and differentiated in hypoxia between days 0 and 8 (vs. maintenance of undifferentiated cells under hypoxia but differentiation under normoxic condition, ie, the exact opposite). Collectively, while the purity and % of PSC-VCMs are comparable, the present yield and efficiency were higher. Although we previously did not report the efficiency, the present protocol provides ~5× more cTNT-positive or PSC-VCMs per PSC. Assuming 300,000 hESCs on day 4, the new protocol generates up to 72 cTNT-positive cells per HES2 cell (vs. 13 cTnT-positive cells per undifferentiated cell). We have now also expanded to include additional lines.

Conclusion

Recent differentiation methods have led to higher CM yields compared to traditional spontaneous differentiation protocols. However, many require optimization of multiple growth factors for different hPSC lines, with variability often seen with hiPSC lines. Our method does not require an optimization between activin-A and BMP4; the same concentrations of activin-A and BMP4 were used for all the different hESC and hiPSC lines tested but both the efficiency for ventricular specification remains consistently high. Further, most data are reported as the percentage of contracting EBs. Since EBs contain non-CMs and single-cell assays were not performed, the ventricular yields are not known. Further, the percent yield of ventricular CMs compared with other chamber-specific types is often not reported. In sum, our protocol reported here represents a cost-effective, reproducible, and straightforward VCM specification method for hESC and hiPSC lines. These results may lead to mass production of hPSC-VCMs on a suitable scalable platform (eg, bioreactors and microcarriers).

Acknowledgments

This work is supported by the following grants: the Research Grant Council (TBRS T13-706/11), GRF (103544), and HKU Small Project Funding (201209176132). The imaging and flow cytometry data were acquired using

equipment maintained by the University of Hong Kong Li Ka Shing Faculty of Medicine Faculty Core Facility.

Author Disclosure Statement

No competing financial interests exist.

References

1. Kattman SJ, AD Witty, M Gagliardi, NC Dubois, M Niapour, A Hotta, J Ellis and G Keller. (2011). Stage-specific optimization of activin/nodal and BMP signaling promotes cardiac differentiation of mouse and human pluripotent stem cell lines. Cell Stem Cell 8:228–240.
2. Zhang J, M Klos, GF Wilson, AM Herman, X Lian, KK Raval, MR Barron, L Hou, AG Soerens, et al. (2012). Extracellular matrix promotes highly efficient cardiac differentiation of human pluripotent stem cells: the matrix sandwich method. Circ Res 111:1125–1136.
3. Yang L, MH Soonpaa, ED Adler, TK Roepke, SJ Kattman, M Kennedy, E Henckaerts, K Bonham, GW Abbott, et al. (2008). Human cardiovascular progenitor cells develop from a KDR+ embryonic-stem-cell-derived population. Nature 453:524–528.
4. Burridge PW, S Thompson, MA Millrod, S Weinberg, X Yuan, A Peters, V Mahairaki, VE Koliatsos, L Tung and ET Zambidis. (2011). A universal system for highly efficient cardiac differentiation of human induced pluripotent stem cells that eliminates interline variability. PLoS One 6:e18293.
5. Burridge PW and ET Zambidis. (2013). Highly efficient directed differentiation of human induced pluripotent stem cells into cardiomyocytes. Methods Mol Biol 997:149–161.
6. Lecina M, S Ting, A Choo, S Reuveny and S Oh. (2010). Scalable platform for human embryonic stem cell differentiation to cardiomyocytes in suspended microcarrier cultures. Tissue Eng Part C Methods 16:1609–1619.
7. Lian X, J Zhang, SM Azarin, K Zhu, LB Hazeltine, X Bao, C Hsiao, TJ Kamp and SP Palecek. (2013). Directed cardiomyocyte differentiation from human pluripotent stem cells by modulating Wnt/beta-catenin signaling under fully defined conditions. Nat Protoc 8:162–175.
8. Kehat I, D Kenyagin-Karsenti, M Snir, H Segev, M Amit, A Gepstein, E Livne, O Binah, J Itskovitz-Eldor and L Gepstein. (2001). Human embryonic stem cells can differentiate into myocytes with structural and functional properties of cardiomyocytes. J Clin Invest 108:407–414.
9. He JQ, Y Ma, Y Lee, JA Thomson and TJ Kamp. (2003). Human embryonic stem cells develop into multiple types of cardiac myocytes: action potential characterization. Circ Res 93:32–39.
10. Mummery C, D Ward-van Oostwaard, P Doevendans, R Spijker, S van den Brink, R Hassink, M van der Heyden, T Opthof, M Pera, et al. (2003). Differentiation of human embryonic stem cells to cardiomyocytes: role of coculture with visceral endoderm-like cells. Circulation 107:2733–2740.
11. Passier R and C Mummery. (2003). Origin and use of embryonic and adult stem cells in differentiation and tissue repair. Cardiovasc Res 58:324–335.
12. Lian X, C Hsiao, G Wilson, K Zhu, LB Hazeltine, SM Azarin, KK Raval, J Zhang, TJ Kamp and SP Palecek. (2012). Robust cardiomyocyte differentiation from human pluripotent stem cells via temporal modulation of canonical Wnt signaling. Proc Natl Acad Sci U S A 109:E1848–E1857.
13. Minami I, K Yamada, TG Otsuji, T Yamamoto, Y Shen, S Otsuka, S Kadota, N Morone, M Barve, et al. (2012). A small molecule that promotes cardiac differentiation of human pluripotent stem cells under defined, cytokine- and xeno-free conditions. Cell Rep 2:1448–1460.
14. Ren Y, MY Lee, S Schliffke, J Paavola, PJ Amos, X Ge, M Ye, S Zhu, G Senyei, et al. (2011). Small molecule Wnt inhibitors enhance the efficiency of BMP-4-directed cardiac differentiation of human pluripotent stem cells. J Mol Cell Cardiol 51:280–287.
15. Elliott DA, SR Braam, K Koutsis, ES Ng, R Jenny, EL Lagerqvist, C Biben, T Hatzistavrou, CE Hirst, et al. (2011). NKX2-5(eGFP/w) hESCs for isolation of human cardiac progenitors and cardiomyocytes. Nat Methods 8:1037–1040.
16. Zhang J, GF Wilson, AG Soerens, CH Koonce, J Yu, SP Palecek, JA Thomson and TJ Kamp. (2009). Functional cardiomyocytes derived from human induced pluripotent stem cells. Circ Res 104:e30–e41.
17. Moore JC, J Fu, YC Chan, D Lin, H Tran, HF Tse and RA Li. (2008). Distinct cardiogenic preferences of two human embryonic stem cell (hESC) lines are imprinted in their proteomes in the pluripotent state. Biochem Biophys Res Commun 372:553–558.
18. Okita K, Y Matsumura, Y Sato, A Okada, A Morizane, S Okamoto, H Hong, M Nakagawa, K Tanabe, et al. (2011). A more efficient method to generate integration-free human iPS cells. Nat Methods 8:409–412.
19. Bates SE. (2011). Classical cytogenetics: karyotyping techniques. Methods Mol Biol 767:177–190.
20. Fu JD, P Jiang, S Rushing, J Liu, N Chiamvimonvat and RA Li. (2010). Na+/Ca2+ exchanger is a determinant of excitation-contraction coupling in human embryonic stem cell-derived ventricular cardiomyocytes. Stem Cells Dev 19:773–782.
21. Chow MZ, L Geng, CW Kong, W Keung, JC Fung, K Boheler and RA Li. (2013). Epigenetic regulation of the electrophysiological phenotype of human embryonic stem cell-derived ventricular cardiomyocytes: insights for driven maturation and hypertrophic growth. Stem Cells Dev 22:2678–2690.
22. Fu JD, SN Rushing, DK Lieu, CW Chan, CW Kong, L Geng, KD Wilson, N Chiamvimonvat, KR Boheler, et al. (2011). Distinct roles of microRNA-1 and −499 in ventricular specification and functional maturation of human embryonic stem cell-derived cardiomyocytes. PLoS One 6:e27417.
23. Swijnenburg RJ, S Schrepfer, JA Govaert, F Cao, K Ransohoff, AY Sheikh, M Haddad, AJ Connolly, MM Davis, RC Robbins and JC Wu. (2008). Immunosuppressive therapy mitigates immunological rejection of human embryonic stem cell xenografts. Proc Natl Acad Sci U S A 105:12991–12996.
24. Cao F, RA Wagner, KD Wilson, X Xie, JD Fu, M Drukker, A Lee, RA Li, SS Gambhir, et al. (2008). Transcriptional and functional profiling of human embryonic stem cell-derived cardiomyocytes. PLoS One 3:e3474.
25. Passier R, DW Oostwaard, J Snapper, J Kloots, RJ Hassink, E Kuijk, B Roelen, AB de la Riviere and C Mummery. (2005). Increased cardiomyocyte differentiation from human embryonic stem cells in serum-free cultures. Stem Cells 23:772–780.
26. Lieu DK, JD Fu, N Chiamvimonvat, KC Tung, GP McNerney, T Huser, G Keller, CW Kong and RA Li.

(2013). Mechanism-based facilitated maturation of human pluripotent stem cell-derived cardiomyocytes. Circ Arrhythm Electrophysiol 6:191–201.
27. Liu J, JD Fu, CW Siu and RA Li. (2007). Functional sarcoplasmic reticulum for calcium handling of human embryonic stem cell-derived cardiomyocytes: insights for driven maturation. Stem Cells 25:3038–3044.
28. Liu J, DK Lieu, CW Siu, JD Fu, HF Tse and RA Li. (2009). Facilitated maturation of Ca2+ handling properties of human embryonic stem cell-derived cardiomyocytes by calsequestrin expression. Am J Physiol Cell Physiol 297: C152–C159.
29. Folmes CD, PP Dzeja, TJ Nelson and A Terzic. (2012). Mitochondria in control of cell fate. Circ Res 110:526–529.
30. Hom JR, RA Quintanilla, DL Hoffman, KL de Mesy Bentley, JD Molkentin, SS Sheu and GA Porter Jr. (2011). The permeability transition pore controls cardiac mitochondrial maturation and myocyte differentiation. Dev Cell 21:469–478.
31. Huang X, L Sun, S Ji, T Zhao, W Zhang, J Xu, J Zhang, Y Wang, X Wang, et al. (2013). Kissing and nanotunneling mediate intermitochondrial communication in the heart. Proc Natl Acad Sci U S A 110:2846–2851.
32. Pohjoismaki JL, M Kruger, N Al-Furoukh, A Lagerstedt, PJ Karhunen and T Braun. (2013). Postnatal cardiomyocyte growth and mitochondrial reorganization cause multiple changes in the proteome of human cardiomyocytes. Mol Biosyst 9:1210–1219.
33. Moore JC, SY Tsang, SN Rushing, D Lin, HF Tse, CW Chan and RA Li. (2008). Functional consequences of overexpressing the gap junction Cx43 in the cardiogenic potential of pluripotent human embryonic stem cells. Biochem Biophys Res Commun 377:46–51.
34. Pearl JI, AS Lee, DB Leveson-Gower, N Sun, Z Ghosh, F Lan, J Ransohoff, RS Negrin, MM Davis and JC Wu. (2011). Short-term immunosuppression promotes engraftment of embryonic and induced pluripotent stem cells. Cell Stem Cell 8:309–317.
35. Karakikes I, GD Senyei, J Hansen, CW Kong, EU Azeloglu, F Stillitano, DK Lieu, J Wang, L Ren, et al. (2014). Small molecule-mediated directed differentiation of human embryonic stem cells toward ventricular cardiomyocytes. Stem Cells Transl Med 3:18–31.

Address correspondence to:
Prof. Ronald A. Li
Stem Cell & Regenerative Medicine Consortium
LKS Faculty of Medicine
The University of Hong Kong
Pokfulam
Hong Kong

E-mail: ronaldli@hku.hk

Dr. Camie W. Chan
Stem Cell & Regenerative Medicine Consortium
LKS Faculty of Medicine
The University of Hong Kong
Pokfulam
Hong Kong

E-mail: camchan@hku.hk

Received for publication October 19, 2013
Accepted after revision February 24, 2014
Prepublished on Liebert Instant Online XXXX XX, XXXX